ACS Photonics

Article

pubs.acs.org/journal/apchd5

# Vertically Stacked Photodetector Devices Containing Silicon Nanowires with Engineered Absorption Spectra

Hyunsung Park[†] and Kenneth B. Crozier*[,†,‡,§]

[†]School of Engineering and Applied Sciences, Harvard University, Cambridge, Massachusetts 02138, United States

[‡]Department of Electrical and Electronic Engineering and [§]School of Physics, University of Melbourne, Melbourne, VIC 3010, Australia

**ABSTRACT:** We fabricate a vertically stacked photodetector device containing silicon nanowire photodetectors formed above a silicon substrate that also contains a photodetector. The nanowire photodetectors have absorption spectra that exhibit peaks for which light is coupled to a waveguide mode, absorbed, and converted to photocurrent. The substrate photodetector converts the light not absorbed by the nanowires to photocurrent. Responsivities of both photodetectors are measured and compared to the predictions of electromagnetic simulations. This device configuration can be thought of as a silicon photodetector with an integrated filter. The filter has the unusual property of converting absorbed light to photocurrent rather than discarding it.

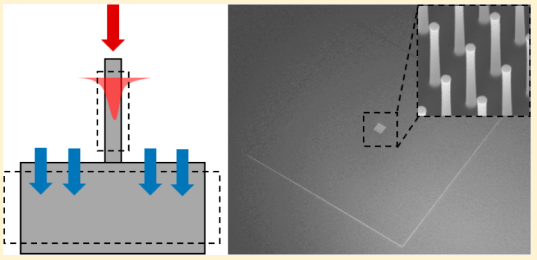

**KEYWORDS:** *silicon nanowires, nanowires, photodetector, stacked photodetector*

A traditional image sensor contains dye-based color filters arranged in a checkerboard pattern between the microlenses and photodetectors. These filters typically transmit red, green, and blue spectral bands, permitting color imaging to be performed. These filters face considerable challenges however in the trend toward ever higher pixel densities that exists at the time of writing.[1] The filters are inherently inefficient, in that they transmit only a portion of the visible spectrum. The current trend toward increasing pixel densities generates the strong need for improved efficiency. This is evidenced by the introduction of back-side illumination devices.[2] In front-side illumination devices, light can be reflected or scattered by the metal interconnection layers. Back-side illumination devices were developed to reduce this source of loss. For the back-side illumination device, the wafer is flipped and substrate is thinned until the photodetectors are exposed. After that, the color filters and microlenses are fabricated on the surface exposed by the thinning process. Back-side illumination allows each pixel to collect more photons because there are no metal layers in the light path.

Although back-side illumination achieves higher efficiency, the color filter still poses a limitation in the scaling down of the pixels. The organic dyes they employ have limited absorption coefficients and are damaged by high temperatures and ultraviolet exposure. Other approaches such as plasmonic color filters are therefore being considered.[1,3] These approaches however share the characteristic that the color filter transmits only part of the spectrum, with other parts being absorbed or reflected. Conversion of this light (that would otherwise be absorbed or reflected) to photocurrent presents a means to increase efficiency. This motivated the proposal of color separations using spectral splitters.[4] Another approach uses the wavelength-dependent absorption length of silicon (Foveon X3 image sensor[5]).

The Foveon X3 image sensor contains three layers of photodetectors, while a conventional image sensor contains a two-dimensional array of photodetectors and color filters. Each pixel of the Foveon X3 image sensor can detect all three primary colors, and there is therefore no need for the interpolation process that causes degradation of image sharpness in conventional image sensors. It has been noted however that the Foveon X3 image sensor has a large overlap in the spectral response of the three channels.[6] In ref 6, the blue photodetector (top photodetector) is shown to have a much wider spectral response than the blue channel of the tristimulus function. Although postprocessing using an appropriate color matrix can generate the correct color, its large off-diagonal terms add noise to the image.[6]

Semiconductor nanowires[7−9] are currently the topic of considerable interest, and it is interesting to consider whether they present opportunities for the challenges faced by image sensor technologies described above. Cao et al. demonstrated that horizontal germanium nanowires have absorption spectra that depend on their radii.[10−12] We demonstrated that etched vertical silicon nanowires exhibit colors because of wavelength-dependent coupling and absorption.[13] Recently, we showed that this effect can be extended to the infrared via germanium nanowires.[14] We demonstrated filters for multispectral imaging by embedding the nanowires into a transparent medium.[15,16] We furthermore demonstrated image sensor pixels comprising nanowires with integrated photodetectors and performed color imaging without additional color filters, i.e., just employing the spectral response of the nanowires themselves.[17] Our nanowire photodetectors have the unusual and technologically useful

**Received:** December 9, 2014
**Published:** March 16, 2015





DOI: 10.1021/ph500463r
*ACS Photonics* 2015, 2, 544−549

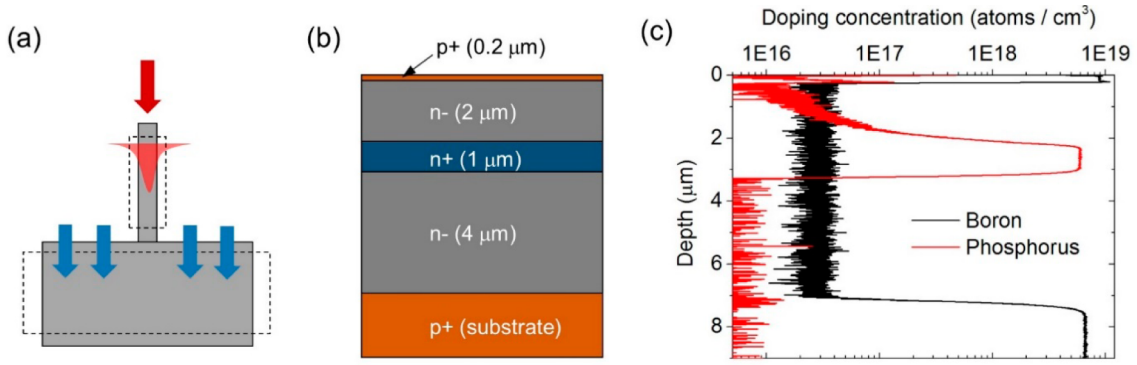


**Figure 1.** (a) Schematic of a vertically stacked photodetector device consisting of silicon nanowires formed above a silicon substrate. (b) Design of epitaxial structure with p+/n−/n+/n−/p+ layers. (c) Depth profile of doping concentration obtained by SIMS.

property that the spectral absorption can be engineered by changing the radii of the nanowires.

Here, we describe the demonstration of a more advanced configuration, in which a second photodetector is added to the substrate, i.e., beneath the nanowires. This could form the basis of an image sensor pixel in which part of the spectrum would be captured by the nanowire photodetector and converted to photocurrent. The remainder of the spectrum would be captured by the substrate photodetector and again converted to photocurrent. In this way, photon capture would be performed in a highly efficient manner, as photons would be not discarded by absorptive filters.

## RESULTS AND DISCUSSION

Figure 1a shows the concept schematic of our device. The nanowire photodetector selectively absorbs part of spectrum, and the substrate photodetector absorbs the light not absorbed by the nanowire. The starting substrate for our device is a silicon wafer on which multiple layers have been grown epitaxially. The use of an epitaxial wafer is motivated by the fact that to collect the photons from the nanowires and the substrate, both parts need to contain p−i−n junctions. As shown in Figure 1b, our multilayered epitaxial wafer contains p+/n−/n+/n−/p+ layers. The nanowire photodetectors are to be fabricated in the top p+/n−/n+ layers. The bottom n+/n−/p+ layers are for the bottom p−i−n junction. Epitaxial wafers are produced by the company IQE Silicon (UK), with the goal being the specifications shown in Figure 1b. The top p+/n−/n+ section thickness is chosen to be 3.2 $\mu$m. This is chosen to match the intended heights of our nanowires. This is in turn dictated by the capabilities of our fabrication process, as to etch nanowires that are taller than this is challenging. For the bottom photodetector, we choose the n-layer to be fairly thick (4 $\mu$m), in order to absorb as much of the light (not absorbed by the nanowires) as possible. We measure the doping profile using secondary ion mass spectrometry (SIMS, performed by Evans Analytical Group USA). The measured depth profile (Figure 1c) generally shows good agreement with the design that was provided to the manufacturer (Figure 1b). The main difference is that rather than being completely abrupt, as indicated in the idealized schematic illustration of Figure 1b, in the actual wafer there are transition regions at the junctions between the layers.

Figure 2a shows the fabrication method of our device. Fabrication begins with etching nanowires using the methods described in our previous paper.[15] It is important, however, that the etching depth be well-controlled to ensure that the resultant nanowires do indeed contain p+/n−/n+ junctions. We therefore choose to etch the nanowires until the middle of the n+ layer. The next step is to define the substrate photodetector. We pattern a thick photoresist (~3.5 $\mu$m thickness). We etch a mesa structure to a depth of ~8 $\mu$m, so that the substrate (p+) is exposed. This defines the substrate photodetector. We use deep reactive-ion etching (DRIE) for this process. The photoresist is then removed by a solvent stripper (PG Remover from MicroChem). The device at this stage consists of etched nanowires formed on a mesa. The nanowires have heights of 2.55 $\mu$m, and the height of the mesa is 8.4 $\mu$m (Figure 2b). Scanning electron micrographs (SEMs) of nanowires with radii of 100 and 120 nm are shown in Figure 2b. We fabricate arrays of 100 × 100 nanowires with a pitch of 1 $\mu$m. We note that the radii mentioned in this paper are the design values employed in the electron beam lithography step. Scanning electron microscopy reveals that the nanowires have some undercut. The third SEM image in Figure 2b shows the mesa structure. The lateral extent of the mesa is 2 mm × 2 mm. This size is chosen to permit PMMA (poly(methyl methacrylate)) spacer fabrication to be carried out. If the mesa is too small, then the PMMA coating will be very nonuniform. Figure 2c shows optical microscope images of the structures comprising nanowire arrays on mesas. It can be seen that the nanowire arrays show colors that depend on the radii of nanowires.[13] To fabricate the top transparent contact, we spin coat PMMA onto the sample. We then place the sample in an oxygen plasma in order to etch the PMMA and expose the tops of the nanowires. An ITO layer is then sputtered on top. We use silver epoxy and gold wires to establish three contacts (ITO, n+, and substrate). The result is shown in Figure 2d. The contact in the bottom left corner of Figure 2d corresponds to the n+ layer contact. This formed by scratching away the PMMA to expose the n+ layer.

The measured $I-V$ curves of our devices without illumination are shown in Figure 3a. We measured $I-V$ characteristics of both the nanowire photodetectors with radii of 100 and 120 nm and the corresponding substrate photodetectors. The photodetectors show the expected diode characteristics. The dark currents of the nanowire and substrate photodetectors at a bias of −1 V range from ~600 pA to ~1 nA. We next measure the responsivities of both the nanowire and substrate photodetectors using the method described in our previous paper.[17] Briefly, light from a quartz tungsten halogen lamp is filtered by a monochromator and focused onto the device using a home-built microscope, with the resultant photocurrent measured by a picoammeter. The optical power impinging on the device is found from measurements performed with a reference photodetector. The responsivities of the photodetectors comprising nanowires with


DOI: 10.1021/ph500463r
ACS Photonics 2015, 2, 544−549

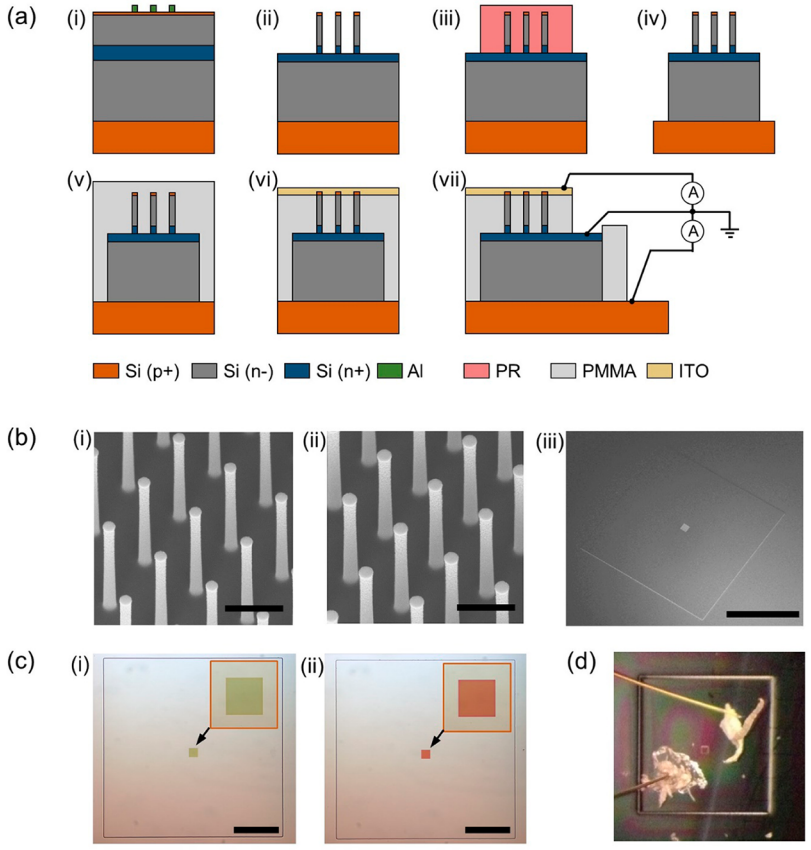


**Figure 2.** (a) Schematic illustration of fabrication method for vertically stacked photodetector device. (i) Aluminum mask is fabricated on the epitaxial wafer. (ii) Dry etching of nanowires. (iii) Photolithography is performed to define the mesa (substrate photodetector). (iv) Dry etching of the mesa. (v) PMMA is spin-coated to make a spacer. (vi) Tops of nanowires are exposed by dry etching of PMMA and ITO is sputtered. (vii) Electrical contacts are established. (b) SEM images of the device after etching nanowires (30° tilted view). (i) Etched nanowires with radii of 100 nm. Scale bar is 1 $\mu$m. (ii) Etched nanowires with radii of 120 nm. Scale bar is 1 $\mu$m. (iii) Etched nanowires on the mesa. Scale bar is 1 mm. (c) Optical microscope images of nanowire arrays fabricated on the mesa. (i, ii) Arrays of nanowires with radii of 100 and 120 nm. Scale bar is 0.5 mm. Insets show magnified view of nanowires area. (d) Photograph of completed device after wire bonding. Contact in bottom left corner is connected to n+. Contact in upper right corner is connected to the ITO layer. Substrate contact is not shown in this picture.

radii of 100 and 120 nm are shown in Figure 3b. It can be seen that each responsivity spectrum shows distinct peaks, whose positions depend on the radii of the nanowires.[17] This effect originates from the wavelength dependence of the field distributions of the guided modes.[13−17] The magnitude of the responsivity is however smaller than that of previous devices.[17] We believe that this is due to the changes in the etching characteristics of the reactive-ion etching (RIE) machine used for this work. These changes to the etching characteristics result in increased damage to the nanowire surface.

The substrate photodetector (Figure 3c) shows responsivity (~0.27 at a wavelength of 630 nm) that can be considered good, although slightly lower than that of a conventional silicon photodetector (e.g., FDS10X10[18] from Thorlabs Inc., with responsivity ~0.4 at $\lambda$ = 630 nm). Modulation of the responsivity spectrum of the substrate photodetector, i.e., ripples, can also be seen. This is because the PMMA film containing the embedded nanowires acts as a Fabry−Perot cavity, resulting in modulation of the spectrum of the light transmitted into the substrate.

Figure 3d shows simulated responsivities. We use the finite-difference time-domain (FDTD) method to calculate the absorption cross sections of both nanowire and substrate photodetectors. We then calculate responsivities with the assumption of 100% internal quantum efficiency. It can be seen that the peak positions of the measured responsivities of the nanowire devices (Figure 3b) are in good agreement with the predictions of simulations (Figure 3d). It should be noted that these simulations are for nanowires whose radii are 35 nm smaller than those of the design values used in the lithography step for the actual device. This trend is consistent with findings of a previous study[17] and could be due to fabrication imperfections, e.g., undercutting during the etching step. It can be seen that the magnitudes of the responsivities of the actual devices (Figure 3b) are considerably (~10 times) lower than the predictions of simulations (Figure 3d). As discussed above, this may be a consequence of recombination at the nanowire surface, a process exacerbated by damage caused by etching. For the substrate detectors, it can be seen that the measurements (Figure 3c) are in good agreement with simulations (Figure 3d) in terms of peak positions as well as the magnitude of the responsivities. Interestingly, it can be seen that for both measurements and simulations substrate photodetector #2 has a responsivity that is suppressed compared to #1 in the spectral range from below 500 nm to approximately 600 nm. This is due to the fact that silicon nanowire array #2 has an absorption peak in this range, thereby reducing the transmission to the substrate photodetector. In other words, the silicon nanowires are acting as optical filters as intended. This filtering effect is not as pronounced as it could be, however, due to the fact that absorption by the nanowires is relatively small (peak value ~20%) in their


DOI: 10.1021/ph500463r
ACS Photonics 2015, 2, 544−549

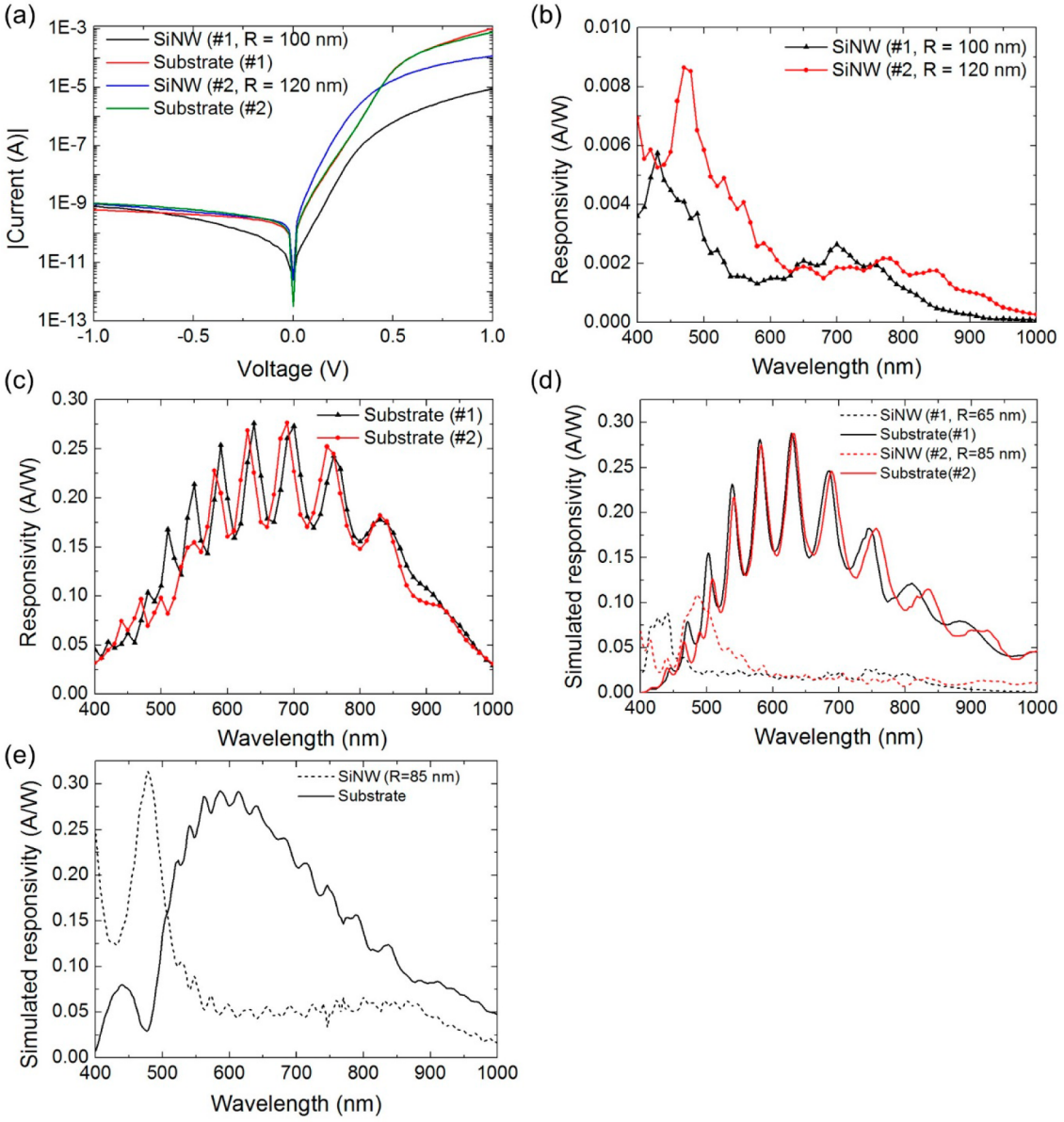


**Figure 3.** (a) Current−voltage characteristics (logarithmic scale) of the fabricated device without illumination. (b) Measured responsivities of photodetectors comprising nanowires with radii of 100 and 120 nm. (c) Measured responsivities of corresponding substrate photodetectors. (d) Simulated responsivities. (e) Simulated responsivities in ideal case ($R$ = 85 nm, 4 $\mu$m tall, 0.7 $\mu$m pitch). ITO layer is removed and thickness of top n+ layer in substrate photodetector is 100 nm.

current configuration. In addition, at shorter wavelengths, incident photons absorbed near the top surface of the substrate photodetector contribute little to the photocurrent due to the highly doped n+ region being relatively thick (400 nm). Furthermore, the ripples in the substrate photodetector's response tend to dominate the response. We next consider a modified design intended to address these issues.

The simulation results for the modified design are shown in Figure 3e. To increase the absorption by the nanowires, they are elongated from 2.55 $\mu$m to 4 $\mu$m, and the nanowire pitch is taken to be 0.7 $\mu$m. The intrinsic region, in which absorbed power is converted to photocurrent, is taken to be 3.45 $\mu$m tall. The nanowires are taken to have radii of 85 nm. As discussed above, the presence of Fabry−Perot fringes in the substrate photodetector response makes the spectral filtering provided by the NWs more difficult to discern. The presence of an antireflection coating would serve to mitigate this. To mimic this function, the simulated device has no ITO layer, and the PMMA is taken to be infinitely thick. It can be seen (Figure 3e) that this greatly reduces the depths of the Fabry−Perot ripples. In addition, we assume the thickness of the n+ regions of the substrate photodetector is 100 nm. Strong peaks appear in the nanowire's simulated responsivity, and corresponding distinct dips can be seen in the substrate's responsivity (Figure 3e). One can regard the power absorbed in the nanowire as being analogous to the power absorbed in a photodetector of an image sensor containing a red-green-blue (RGB) Bayer filter. Similarly, the spectrum of power absorbed in the substrate can be thought of as analogous to the power absorbed in a photodetector of an image sensor containing a cyan-magenta-yellow (CMY) filter. This approach should thus permit color imaging to be performed with high efficiency. To demonstrate this, we perform FDTD simulations.



DOI: 10.1021/ph500463r
*ACS Photonics* 2015, 2, 544−549

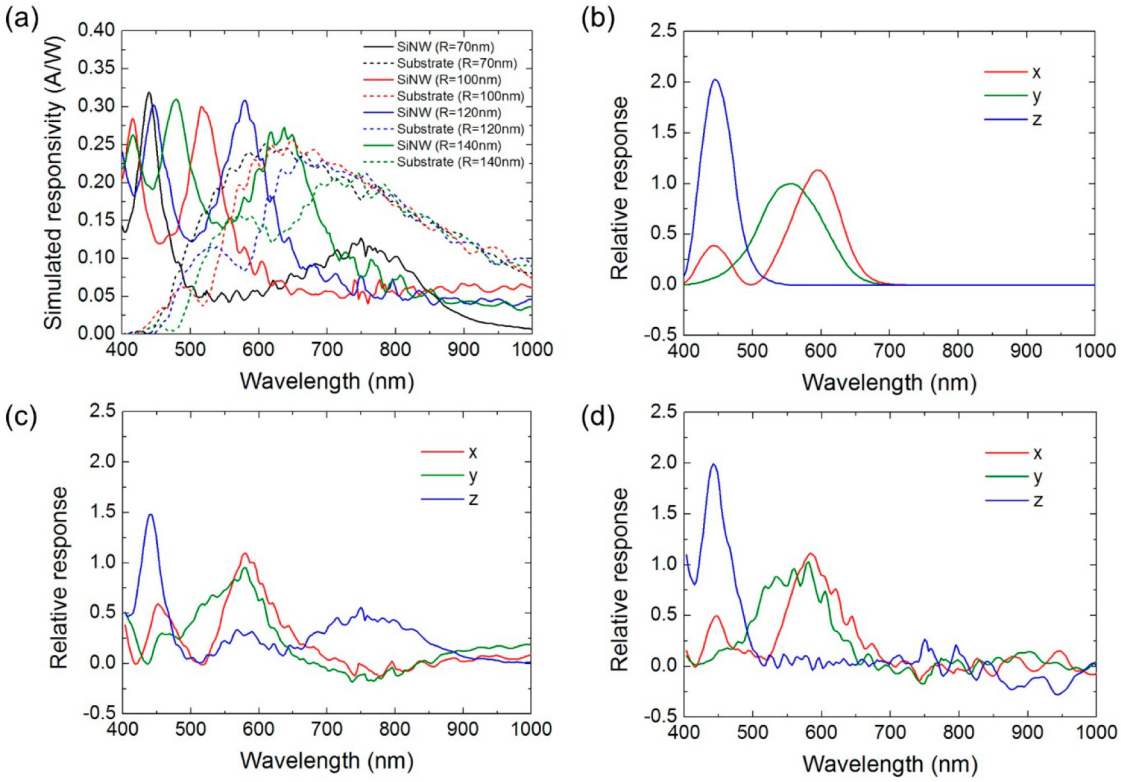


**Figure 4.** (a) Simulated responsivities of nanowire arrays and corresponding substrate photodetectors ($R$ = 70 nm, 100 nm, 120 nm, 140 nm). (b) CIE 1964 XYZ color matching functions. (c) Response functions obtained by linear combination of responsivities of four silicon nanowire arrays. (d) Response functions obtained by linear combination of responsivities of four silicon nanowire arrays and four silicon substrate photodetectors.

Figure 4a shows the simulation results of responsivities for four nanowire arrays and their corresponding substrate photodetectors. The arrays contain nanowires that are 4 $\mu$m tall and on a 0.7 $\mu$m pitch. The simulated devices have no ITO layer, and the nanowires are embedded in PMMA that is infinitely thick. The thickness of the top n+ layer of the substrate photodetector is 400 nm. Figure 4b shows the CIE 1964 XYZ color matching functions.[19] We use the least-squares method to find the linear combination of the four nanowire arrays (Figure 4a) that produces the response most similar to that of the standard color response (Figure 4b). The results are shown in Figure 4c. We repeat this process, this time including not only the four nanowire arrays, but also the four corresponding substrate photodetectors. The results are shown in Figure 4d. Interestingly, the color response obtained when the substrate photodetectors are included (Figure 4d) is closer to the standard color response than that achieved with the nanowire photodetectors only (Figure 4c). In addition, the result shows that no additional filters (i.e., IR cut filter) would be needed for the color imaging. It is seen that the substrate photodetectors are helpful not only for improving photon collection efficiency but also for higher color accuracy.

## CONCLUSION

In conclusion, we fabricated a vertically stacked photodetector device comprising silicon nanowires, each containing a photodetector, formed above a substrate that also contains a photodetector. The measured responsivities show that nanowire and substrate photodetectors each absorb parts of the illumination spectrum. Our approach enables us to collect photons (i.e., absorb and convert to photocurrent) that would otherwise be discarded by conventional color filters.

## AUTHOR INFORMATION

### Corresponding Author

*E-mail: kcrozier@unimelb.edu.au. Tel: +61-3-8344-2249.

### Notes

The authors declare no competing financial interest.

## ACKNOWLEDGMENTS

This work was supported in part by the National Science Foundation (NSF, grant no. ECCS-1307561), by the Australian Research Council's Discovery Projects funding scheme (project number DP150103736), and by the Victorian Endowment for Science, Knowledge and Innovation (VESKI). Fabrication work was performed at the Center for Nanoscale Systems (CNS) at Harvard, which is supported by the NSF.

## REFERENCES

(1) Yokogawa, S.; Burgos, S. P.; Atwater, H. A. Plasmonic color filters for CMOS image sensor applications. *Nano Lett.* **2012**, *12*, 4349−4354.

(2) Pain, B.; Cunningham, T.; Nikzad, S.; Hoenk, M.; Jones, T.; Wrigley, C.; Hancock, B. A back-illuminated megapixel CMOS image sensor. *Proc. 2005 IEEE Workshop CCD Adv. Image Sens.* **2005**, 35−38.

(3) Xu, T.; Wu, Y.-K.; Luo, X.; Guo, L. J. Plasmonic nanoresonators for high-resolution colour filtering and spectral imaging. *Nat. Commun.* **2010**, *1*, 59.

(4) Nishiwaki, S.; Nakamura, T.; Hiramoto, M.; Fujii, T.; Suzuki, M.-A. Efficient colour splitters for high-pixel-density image sensors. *Nat. Photonics* **2013**, *7*, 248−254.

(5) Foveon Inc. (Santa Clara, CA, USA), http://www.foveon.com/article.php?a=69 (accessed February 23, 2015).

(6) Gilblom, D. L.; Yoo, S. K.; Ventura, P. Operation and performance of a color image sensor with layered photodiodes. *Proc. SPIE 5074* **2003**, 318−331.



DOI: 10.1021/ph500463r
*ACS Photonics* 2015, 2, 544−549

(7) Xia, Y.; Yang, P.; Sun, Y.; Wu, Y.; Mayers, B.; Gates, B.; Yin, Y.; Kim, F.; Yan, H. One-dimensional nanostructures: synthesis, characterization, and applications. *Adv. Mater.* **2003**, *15*, 353−389.
(8) Hu, J.; Odom, T. W.; Lieber, C. M. Chemistry and physics in one dimension: synthesis and properties of nanowires and nanotubes. *Acc. Chem. Res.* **1999**, *32*, 435−445.
(9) Fan, Z.; Razavi, H.; Do, J.-W.; Moriwaki, A.; Ergen, O.; Chueh, Y.-L.; Leu, P. W.; Ho, J. C.; Takahashi, T.; Reichertz, L. A.; Neale, S.; Yu, K.; Wu, M.; Ager, J. W.; Javey, A. Three-dimensional nanopillar-array photovoltaics on low-cost and flexible substrates. *Nat. Mater.* **2009**, *8*, 648−653.
(10) Cao, L.; Fan, P.; Barnard, E. S.; Brown, A. M.; Brongersma, M. L. Tuning the color of silicon nanostructures. *Nano Lett.* **2010**, *10*, 2649−2654.
(11) Cao, L.; Park, J.-S.; Fan, P.; Clemens, B.; Brongersma, M. L. Resonant germanium nanoantenna photodetectors. *Nano Lett.* **2010**, *10*, 1229−1233.
(12) Cao, L.; White, J. S.; Park, J.-S.; Schuller, J. A.; Clemens, B. M.; Brongersma, M. L. Engineering light absorption in semiconductor nanowire devices. *Nat. Mater.* **2009**, *8*, 643−647.
(13) Seo, K.; Wober, M.; Steinvurzel, P.; Schonbrun, E.; Dan, Y.; Ellenbogen, T.; Crozier, K. B. Multicolored vertical silicon nanowires. *Nano Lett.* **2011**, *11*, 1851−1856.
(14) Solanki, A.; Crozier, K. B. Vertical germanium nanowires as spectrally-selective absorbers across the visible-to-infrared. *Appl. Phys. Lett.* **2014**, *105*, 191115.
(15) Park, H.; Crozier, K. B. Multispectral imaging with vertical silicon nanowires. *Sci. Rep.* **2013**, *3*, 2460.
(16) Park, H.; Seo, K.; Crozier, K. B. Adding colors to polydimethylsiloxane by embedding vertical silicon nanowires. *Appl. Phys. Lett.* **2012**, *101*, 193107.
(17) Park, H.; Dan, Y.; Seo, K.; Yu, Y. J.; Duane, P. K.; Wober, M.; Crozier, K. B. Filter-free image sensor pixels comprising silicon nanowires with selective color absorption. *Nano Lett.* **2014**, *14*, 1804.
(18) Thorlabs Inc. (Newton, NJ, USA), https://www.thorlabs.com/thorcat/24700/FDS10X10-SpecSheet.pdf (accessed Feburary 23, 2015).
(19) Wyszecki, G.; Stiles, W. S. *Color Science: Concepts and Methods, Quantitative Data and Formulae*; Wiley: New York, 1982.



DOI: 10.1021/ph500463r
*ACS Photonics* 2015, 2, 544−549